Rydberg states in multiphoton atomic ionization processes

G. K. Ivanov, G. V. Golubkov, and D. M. Manakov

N. N. Semenov Institute of Chemical Physics, Russian Academy of Sciences, 117977 Moscow, Russia
(Submitted 15 June 1994; resubmitted 20 July 1994)
Zh. Eksp. Teor. Fiz. **106**, 1306–1318 (November 1994)

We investigate the emergence of Rydberg states resulting from resonant multiphoton ionization induced by the linearly polarized monochromatic field produced by a high-power laser. We employ the radiative collision matrix method to analyze multiphoton ionization in which a Rydberg state becomes ionized prior to a resonant transition from a low-lying p state populated by absorption of a photon from a weak (probe) field. We carefully examine the situation in which an s and d state that are strongly coupled to the p state, and which are degenerate in l, give rise to two new mixed states. Only one of the latter exhibits levels that are strongly shifted and narrowed as the (moderate) field strength increases (stabilization effect). Simple analytic expressions are obtained to illustrate the spectral properties of the photoelectrons coming from these hybrid states. We show that due to field coupling via the continuum, at energies $E=\omega_f-1/(2n^2)$, electrons with high angular momentum $l\leqslant(3/\omega_f)^{1/3}$ can be produced near threshold, where relatively few photons $\hbar\omega_f$ are absorbed from the strong field. As an application of the theory developed here, we calculate the field-strength dependence of the autoionized widths of the Rydberg levels of a hydrogen atom induced by an external field, and the field-strength dependence of the corresponding quantum defects. © *1994 American Institute of Physics.*

1. INTRODUCTION

This paper deals with the role played by Rydberg states and by the specifics of their emergence in multiphoton atomic ionization processes induced by a strong electromagnetic field. Because of Coulomb crowding of the atomic levels and multiple degeneracy, Rydberg states behave in an electromagnetic field entirely differently from discrete states well-separated in energy.

An interesting phenomenon stems from the first of these properties, namely the stabilization of highly excited states, i.e., a decrease in the width Γ_n of the Rydberg states with increasing external field strength (n is the principal quantum number of an atomic level). Due to the accidental degeneracy in orbital angular momentum l associated with the Coulomb interaction (which exists for all feasible l in a hydrogen atom, and in fact for $l>2$ in other atoms and simple molecules), the system considered here can give rise to distinctive "hybrid" mixed states that are responsible for migration of the electron population in l. Under certain conditions, this can lead in turn to the efficient production of high-l photoelectrons in processes in which relatively few (k) photons are absorbed from the strong field, i.e., $k<l$.

A number of recent papers[1–4] have reported numerical modeling of multiphoton processes involving atomic Rydberg states. Note that in extremely strong fields ($f>1$, where f is the field strength in atomic units, with $\hbar=m_e=e=1$), such calculations are probably the only possible way to solve the problem. But in moderate electromagnetic fields for which the amplitude $f\omega_f^{-2}$ of classical electron oscillations at frequency ω_f is small compared with the wavelength λ, the analytic possibilities of the theory are far from exhausted. This is particularly true when the dipole transition amplitude between continuum states in a Coulomb potential is small, i.e.,

$$f\omega_f^{-5/3}\ll 1. \tag{1}$$

In the present paper, we use (1) to derive the analytic behavior of the photoelectron spectrum for several experimentally realizable photoprocesses. The need to view them in the light of previous theoretical investigations (see the appropriate sections in Refs. 5–7, along with the original papers[8,9]) derives above all from the fact that the electromagnetically induced deexcitation of Rydberg states depends on the way in which they have been prepared. We point out that in the analytically tractable problem of atomic deexcitation from a Rydberg state fixed at $t=0$, stabilization occurs only in superstrong field.[7,10,11] At the same time, in the resonant excitation of the $n,l+1$ and $n,l-1$ states from a low-lying $n_0 l$ state (with $n\gg n_0$), stabilization is also possible in moderate fields, with $f^2/(n_0^3|E_n-E_{n_0}-\omega_f|)\cong 1$.[12] This is not purely an interference effect here, but has to do with the quantum defect μ induced by the laser in the Rydberg state undergoing deexcitation, i.e.,

$$\Gamma_n=\Gamma_n^0\cos^2\pi\mu, \tag{2}$$

where Γ_n^0 is the field width in the absence of resonance. According to Ref. 12, μ depends on the field interaction between $n_0 l$ and the $n,l+1$ and $n,l-1$ states, and on the position of the Rydberg state E_n relative to $E_{n_0}+\omega_f$. The behavior of (2) as a function of the strength f of a monochromatic field is such that $\Gamma_n\propto f^2$ in low fields, it reaches some maximum, and it then falls off as $\Gamma_n\propto 1/f^2$.

Both effects and their visible manifestations in the spectrum of photoelectrons with various angular momenta can be

 1063-7761/94/110707-07$10.00

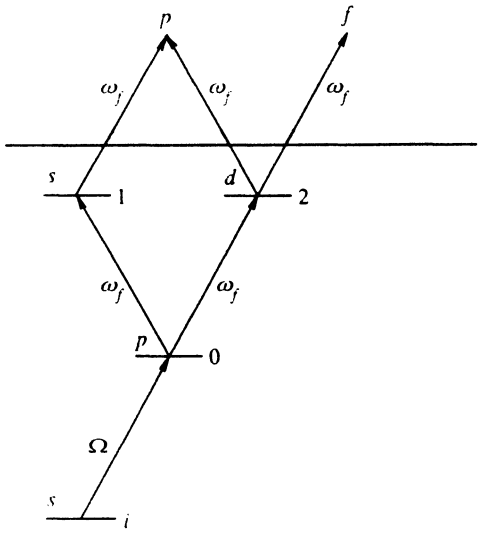

FIG. 1. Photoionization diagram for atomic hydrogen.

studied for the transition schemes in Figs. 1 and 2, in which the Rydberg states partaking in the process are excited via a resonant transition from a low-lying intermediate $n_0 l$ state that has been populated by absorption of a weak-field (probe) photon Ω.

Our method of solution differs from the conventional approach to the theory of multiphoton ionization, in which one writes out and solves the equations for the populations of the individual states, assuming that the effective interaction field acting between them has been turned on instantaneously. In our approach, we take advantage of the possibility of reducing the Schrödinger equation for a system subject to time-periodic excitation to a set of time-independent equations;[6] this approach can be implemented (in contrast to the approach taken in Ref. 13, for example) using integral equations for the scattering problem in which the boundary

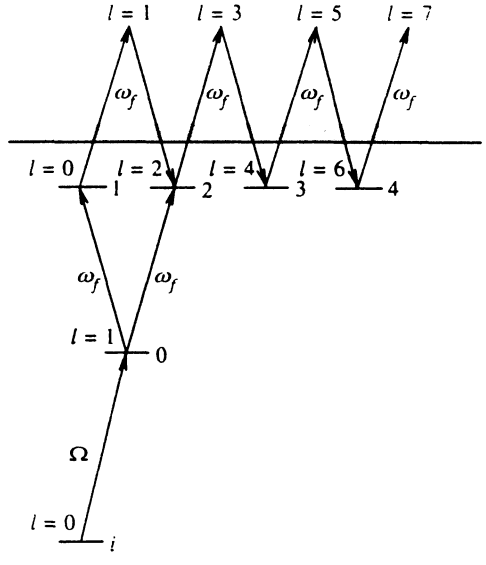

FIG. 2. Expanded photoionization diagram with population diffusion in l.

conditions are automatically taken into account when the inequality (1) holds.

We also show that the steady-state radiative collision matrix method[12,14–16] can be applied to multiphoton ionization processes when the intermediate state is first excited by a weak (probe) field. The ionization probability and the photoelectron spectrum can then be expressed in terms of the scattering amplitude of the ionization products, i.e., electrons and ions in a strong radiation field. We illustrate the theory by treating the hydrogen atom and atoms of the alkali metals.

2. THE RADIATIVE COLLISION MATRIX METHOD IN THE THEORY OF MULTIPHOTON IONIZATION

The transition probability amplitude for the process depicted in Fig. 2 can be calculated in first-order perturbation theory in terms of the weak-field interaction

$$A_{if}=\langle\Psi_i|\hat{\mathbf{D}}|\Psi_E\rangle, \tag{3}$$

where $\hat{\mathbf{D}}$ is the dipole moment operator, Ψ_i is the wave function of the initial state i, and Ψ_E is the electron wave function in the continuous spectrum of an e^-+A^+ system in the presence of an intense field at frequency ω_f. The electron energy in the vicinity of the threshold is

$$E'=2\omega_f+\Omega-I_0 \tag{4}$$

(I_0 is the ionization potential).

To construct the wave function Ψ_E, we begin with the solution of the inverse problem for slow electron scattering from an A^+ ion bathed in an intense radiation field at frequency ω_f. To relate this problem to multiphoton ionization, it will be necessary to deal with the entire set of states interacting via this field.

For an e^-+A^+ system that is not in an external field, one normally introduces Rydberg states plus low-lying discrete atomic states s (with wave functions $|s\rangle$ normalized to unity) that are not subject to the rules governing the Rydberg states. For the Rydberg states, the quantum defects μ_l are assumed to be independent of the energy ε. It is well known that when $r|\varepsilon|\ll 1$ (where the energy $|\varepsilon|\ll 1$), the energy-normalized wave functions of the discrete and continuous spectrum of a Rydberg electron with the same quantum numbers l_m can be effectively be viewed as describing a single electron state (in the latter, the quantum number m, which is unchanged when l is projected on the quantization axis $\mathbf{f}$, is dropped).

For collisions that take place in an intense monochromatic radiation field (with frequency ω_f and amplitude f), one can make use of the idea of quasienergetic harmonics, the levels (or terms) of which have been shifted relative to on another by k, where k characterizes the change in the number of photons ($k<0$ corresponds to a decrease, i.e., to absorption). A relationship exists between the states k and $k\pm 1$ by virtue of the interaction

$$V^f=-(\mathbf{rf})/2, \tag{5}$$

where $\mathbf{r}$ is the radius vector of the isolated electron.

The basis functions are now the wave functions $|g\rangle$ of the Rydberg channels [which are independent of k; here $g=(l,k)$] and the $|s_k\rangle$, which are defined for energies

$$E_k=E-k\omega_f, \tag{6}$$

where E is the energy of the system after absorbing a primary photon Ω.

The equation for the $\mathbf{T}$ matrix, which describes radiative collisions in the e^-+A^+ system as the Rydberg states $|g\rangle$ and a set of low-lying atomic states $|s_k\rangle$ is populated at some intermediate stage, is[12,16]

$$\mathbf{T}=\mathbf{t}+\mathbf{t}\sum_g |g\rangle\langle g|\cot\,\pi(\nu_k+\mu_l)\mathbf{T}$$

$$+\mathbf{t}\sum_{s,k} |s_k\rangle\langle s_k|/(E-k\omega_f-E_s)\mathbf{T}, \tag{7}$$

where $\nu_k=[2(k\omega_f-E)]^{-1/2}$ is the effective principal quantum number of the Rydberg state in the gth channel (when $k\omega_f<E$, $\cot\,\pi\nu_k=-i$), and E_s is the energy of the level s. The t operator, which is a smooth function of energy, satisfies the equation

$$\mathbf{t}=V^f+V^f\sum_k \tilde{\mathbf{G}}(E-k\omega_f)V^f=V^f\tilde{\Omega}, \tag{8}$$

in which $\tilde{\mathbf{G}}(E)$ is the Green's function of the e^-+A^+ system with the field interaction V^f turned off and the pole singularities taken in account in (7) excluded. When Eq. (1) holds, an iterative procedure will necessarily determine $\mathbf{t}$, with the Stark shifts of the levels being incorporated to second order in the perturbation V^f.

Equation (7) can be applied directly to determine the wave functions Ψ_p in (4):

$$\Psi_p=\Phi_p+\sum_g \Phi_g\,\cot\,\pi(\nu_k+\mu_l)T_{gp}$$

$$+\sum_{s,k} \Phi_{s_k}T_{s_kp}/(E-k\omega_f-E_s). \tag{9}$$

The latter can be expressed in terms of the elements of the $\mathbf{T}$ matrix and the so-called modified states, which are real functions that represent states "dressed" by the interactions V^f. These states can be concocted, using the operator $\tilde{\Omega}$, from the basis functions represented in the Green's function $\tilde{G}$ in (8):

$$\Phi_g=\tilde{\Omega}|q\rangle, \quad \Phi_{s_k}=\tilde{\Omega}|s_k\rangle.$$

Making use of (7) and (8) to calculate the matrix elements of (4), and noting that photoabsorption at frequency Ω takes place at a fixed value of k ($k=0$ for processes modeled after Fig. 1, if we ascribe the value $k=-2$ to those electrons near threshold that go off to infinity), we have for the transition amplitude to the p continuum ($p=l,k$) with $E>k\omega_f$

$$M_{ip}=\langle\Psi_i|\hat{\mathbf{D}}|\Psi_0\rangle B_{0p}, \tag{10}$$

where $B_{0p}=T_{0p}(E-E_0)^{-1}$, and Ψ_0 and E_0 are the wave function and energy of the intermediate s_k state at $k=0$.

Equations (7), (9) and (10) describe photoionization under continuous illumination conditions, wherein an electron is excited to the first intermediate level by the weak field, but one nevertheless allows for a full cascade of radiative transitions induced by the strong field.

Time-dependent equations for the level populations and equations for the density matrix are both widely utilized in the theory of multiphoton ionization.[5–7] Analysis has shown that the results obtained with the aid of the time-independent equations (7)–(9) is completely equivalent to the time-dependent approach if one assumes that a system in an intermediate level 0 is subject to the uninterrupted influence (after the source is turned on at $t=0$) of a monochromatic field with constant amplitude f. Note that it is also easy to take relaxation associated with spontaneous emission into account in Eqs. (7)–(9), but we ignore any interaction between the atoms or molecules and the ambient medium.

According to (10), the photoelectron spectrum in the p continuum is proportional to the square of the matrix element $T_{\rm op}$, which can be obtained from (7). The rank of T_{0p} can be reduced to the number of discrete states s_k and closed Rydberg channels that it contains ($c=g$ for $E<k\omega_f$), i.e.,

$$\mathbf{T}=\mathbf{T}'+\mathbf{T}'\sum_c |c\rangle\langle c|\cot\,\pi(\nu_k+\mu_l)\mathbf{T}$$

$$+\mathbf{T}'\sum_{s,k} |s_k\rangle\langle s_k|\mathbf{T}/(E-k\omega_f-E_s), \tag{11}$$

if we introduce the auxiliary operator[16]

$$\mathbf{T}'=\mathbf{t}-i\mathbf{t}\sum_p |p\rangle\langle p|\mathbf{T}'. \tag{12}$$

In contrast to (7), the sum on the right-hand side of (12) is taken only over states in open p channels.

Equation (12) can be used immediately to build the matrix T_{0p}, which couples states in closed and open channels. When we do so, the algebraic equations for T_{s_kp} and T_{cp} will contain two types of matrix elements, T'_{s_kp} and T'_{cp}. In the weak-coupling approximation for the open channels, i.e., when (1) holds, we can approximate the effective interactions between states in the closed channels with expressions of the form

$$T'_{ss'}\approx t_{ss'}-i\sum_p t_{sp}t_{ps'}=t_{ss'}-i\gamma_{ss'}, \tag{13}$$

the structure of which is analogous to the corresponding matrix elements in the time-dependent method of Ref. 17. We can identify the matrix elements $T'_{cp}\approx t_{cp}$ with the partial halfwidths Γ_n of the quasidiscrete levels. For the Rydberg states in particular,

$$E^r_n=k\omega_f-1/(2(n-\mu)^2)-i\sum_p |t_{cp}|^2/(\pi n^3). \tag{14}$$

3. PHOTOIONIZATION IN THE RESONANT EXCITATION OF TWO SERIES OF RYDBERG STATES

We consider a hydrogen atom in which the n_0p state 0, which is populated by transitions from the ground state induced by a weak field (frequency Ω), is mixed upon reradiation of strong-field photons with two Rydberg states belonging to the s- and d-series. Below p, s, and d are denoted by indices 0, 1, and 2, respectively. For transition s to the p- and f-continua, which interact directly with the excited Rydberg states, the weak coupling to states with $l=4$ and 6 can be neglected.

We then obtain for the transition amplitude T_{0p} in (10), making use of (7),

$$T_{0p}=\frac{Qz+iR}{(z-a+i\gamma_\Sigma)(z+i\tilde{\gamma})}, \tag{15}$$

where

$$z=\tan \pi\nu, \quad Q=t_{01}t_{1p}+t_{02}t_{2p},$$

$$R=t_{02}t_{2p}\gamma_1+t_{01}t_{1p}\gamma_2+(t_{01}t_{2p}+t_{02}t_{1p})\gamma_{12},$$

$$\gamma_s=\gamma_{ss},$$

$$a=\frac{t_{01}^2+t_{02}^2}{\varepsilon_0}, \quad \gamma_\Sigma=\gamma_1+\gamma_2-\tilde{\gamma},$$

$$\tilde{\gamma}=\frac{t_{01}^2\gamma_2+t_{02}^2\gamma_1+2t_{01}t_{02}\gamma_{12}}{t_{01}^2+t_{02}^2} \tag{16}$$

($\varepsilon_0=E-E_0$ is the instantaneous value of the energy relative to E_0, and ν is defined by $-1/2\nu^2=E+\omega_f=E'-\omega_f$). According to (11), two types of hybrid states show up in the spectra, and these exhibit markedly different characteristics when $a\gg 1$.

In the first, there is an unmistakable stabilization effect, since as the quantum defect induced by the field increases, $\mu\to\pm 1/2$, the width $\Gamma_n=(\gamma_\Sigma/\pi n^3)\cos^2\pi\mu$ obtained from the equation $z-a+i\gamma_\Sigma=0$ tends to zero. Because $a\sim\gamma_\Sigma/\pi n_0^3\varepsilon_0$, in moderate fields (1) it grows quite large, due to the fact that $n\gg n_0$.

Here (i.e., $z\approx a$) B_{op}, as defined in (10), turns out to be

$$B_{0p}=\frac{1}{\varepsilon_0}\frac{Q}{z-a+i\gamma_\Sigma} \tag{17}$$

and a clearcut series of Rydberg resonances shows up in the spectrum,

$$W(E)_1=\sum_n I_n\frac{1}{\pi}\frac{\Gamma_n}{(E-E_n)^2+\Gamma_n^2}. \tag{18}$$

It can easily be shown that the line intensities at $E'\approx E_n=\omega_f-1/2(n-\mu)^2$

$$I_n=\frac{1}{\nu^3}V_{i0}^2\frac{Q^2}{\gamma_\Sigma[\varepsilon_0^2+(t_{01}^2+t_{02}^2)]} \tag{19}$$

decrease as the perturbed Rydberg level migrates away from the resonance $E_0+\omega_f(\varepsilon_n=E_n-E_0-2\omega_f)$.

The second type of restructured Rydberg state responds weakly to a resonant perturbation. We then have

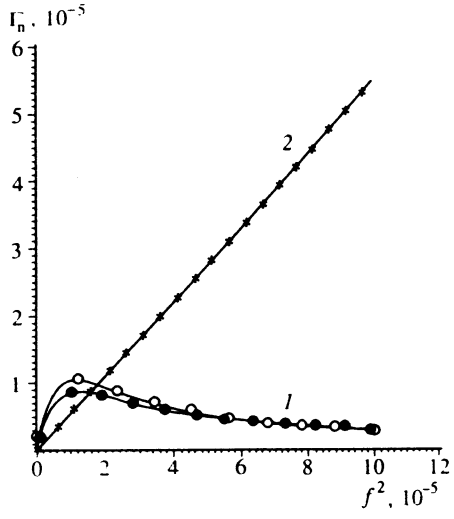

FIG. 3. Field-induced Rydberg level width Γ_n ($n=9$) as a function of f^2. *1*—Strongly perturbed hybrid states ○—exact solution ●—solution given by Eq. (2) *2*—Weakly perturbed hybrid states

$$B_{0p}=-\frac{Qz+iR}{(t_{01}^2+t_{02}^2)(z+i\tilde{\gamma})}, \tag{20}$$

i.e.,

$$|B_{0p}|^2=\frac{R^2}{(t_{01}^2+t_{02}^2)^2} \quad \text{for } z=0,$$

and

$$|B_{0p}|^2=\frac{Q^2}{(t_{01}^2+t_{02}^2)} \quad \text{for } z\approx a.$$

These states show up as a modest singularity against a background set by a weakly energy-dependent process. For $R/\tilde{\gamma}<Q$, this singularity is effectively an antiresonance.

Note that the existence of a huge nonresonant scattering background stems from the striking rearrangement of the roles played by strongly and weakly perturbed atomic Rydberg states in photoionization scheme considered here.

By way of illustration, we have used the foregoing method to calculate numerically the widths (see Fig. 3) and induced quantum defects (see Fig. 4) of the Rydberg states of a hydrogen atom excited via the scheme shown in Fig. 1 (with a strong-field frequency $\omega_f=0.12$). The two plots confirm the hybridization behavior described above, the net result being that one level is significantly split and stabilized, while the other behaves in the usual way. Furthermore, at the point at which stabilization is actually observed, the width of the second level is greater than that of the stabilizing level, which means that we are dealing with "partial" stabilization.

Note that an excitation scheme for coupling Rydberg states not just via the common continuum, but via a low-lying coupled state as well has a number of advantages. For example, much lower intensities are required than in more traditional systems[10] to produce stabilization.

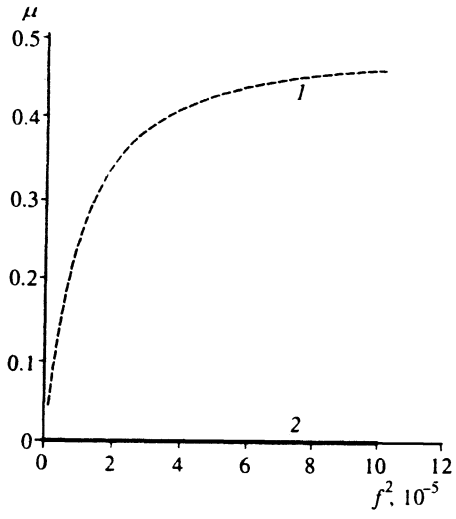

FIG. 4. Field-induced quantum defects as a function of f^2 for strongly (*1*) and weakly (*2*) perturbed Rydberg states.

4. PRODUCTION OF PHOTOELECTRONS WITH HIGH ANGULAR MOMENTUM VIA RESONANT EXCITATION OF SINGLY DEGENERATE ATOMIC RYDBERG STATES

We can make the transition scheme considered above somewhat more comprehensive by incorporating states with high angular momentum l that are populated via the continuum (see Fig. 2). The p and s states and the p and d states then turn out to be strongly coupled. The remainder (including those with $l>2$) are only weakly coupled to one another, since in the first instance the interaction is linear in the field f, and in the second, it is quadratic.

We note that the influence of the coupling of $nl,nl+2$, etc. states via the continuum has been discussed in the literature in connection with the migration of populations. In Ref. 18, for example, the authors addressed the temporal evolution of l levels from a p state prescribed at $t=0$. The simplest imaginable theoretical model was employed in that paper (involving system characteristics that are independent of l), and the photoelectron spectrum was not considered at all.

The present problem involves a different photoionization scheme from that in Ref. 18: it entails an analytic investigation of the spectral features of high-l photoelectrons geared to elucidating the most favorable conditions for experimental observations.

The coupling between l states of the same parity is given by Eq. (13), where we can put

$$t_{l,l+2}\approx -i\gamma_{l,l+2}=-it_{l,l+1}t_{l+1,l+2}. \tag{21}$$

Obviously there will also be real corrections to this term due to virtual transitions via $l+1$ states included in the definition of the Green's function $\tilde{G}$ in Eq. (8). In actual practice,[7] however, these corrections are usually an order of magnitude smaller than the term shown in (21). For simplicity, we also neglect the dynamic Stark shifts contained in the second term of Eq. (8) (these are normally smaller than the widths already considered, and can easily be subsumed into the latter as a parameter of the theory).

Under resonant conditions in nl levels (with various values of l), s and d states populated via a resonant transition from an intermediate p level can become the origin of a transition cascade leading to the migration of populations with $l>2$ (see Fig. 2). According to dipole-transition selection rules, each of these states will decay to near-threshold continua, with an increase or decrease in l.

Below we consider a five-level system (Fig. 2) containing a lowest-lying p level, which by virtue of the reradiation of external field photons is strongly coupled to s and d states in resonance with a series of weakly interacting states with $l=4$ and $l=6$. These we assign subscripts 3 and 4 (as before, the p, s, and d states are denoted by 0, 1, and 2).

Solving the inhomogeneous algebraic equations derived from (11), we obtain the following results. As before, the neighborhood of a strongly perturbed (stabilized) Rydberg resonance can be described by (17). Only photoelectrons with $l=1$ or $l=3$ are efficiently produced here. Substantially new features show up for resonances that produce unperturbed levels at $z\approx 0$. In this spectral range, photoelectrons with $l=1$ and $l=3$ are described by a formula virtually identical to (20). The formula describing the influence of closed Rydberg channels with $l=4$ and $l=6$ is too involved to reproduce here. The expressions for high angular momentum photoelectrons with $l\geqslant 5$ are more transparent:

$$B_{0p}^{(l=5)}=\frac{(t_{01}t_{12}-t_{02}\tilde{z}_1)t_{23}(t_{4p}t_{34}-t_{3p}\tilde{z}_4)}{\mathrm{Det}},$$

$$B_{0p}^{(l=7)}=\frac{(t_{01}t_{12}-t_{02}\tilde{z}_1)t_{23}t_{34}t_{45}}{\mathrm{Det}}, \tag{22}$$

where for the present region $z\approx 0$, the system determinant is

$$\mathrm{Det}=-(t_{01}^2+t_{02}^2)[(z+i\gamma_4)((z+i\tilde{\gamma})(z+i\gamma_3)+b) - t_{34}^2(z+i\tilde{\gamma})] \tag{23}$$

and

$$\tilde{z}_j=z+i\gamma_j,\quad b=\frac{t_{23}^2t_{01}^2}{t_{01}^2+t_{02}^2},\quad t_{j,j+1}=-i\gamma_{j,j+1}.$$

It is of interest to track the behavior of the photoelectron spectra as l increases. At energies near the unperturbed Coulomb levels $E'=\omega_f-1/(2n^2)$, photoelectrons with $l=1$ and $l=3$ have no clearcut resonant behavior, since as we noted above [see Eq. (20)], for $z=\tan\pi\upsilon\gg\gamma$, $|T_{0p}^{l=1,3}|^2$ tends to a constant value, while for states with $l=2m+1=5,7,9,$

$$|T_{0p}^{2m+1}|^2\sim\frac{1}{z^{2m-2}}.$$

The line intensity decreases with increasing l for $l\geqslant 5$, but the decrease is fairly smooth,

$$\frac{|T_{0p}^{l+2}|^2}{|T_{0p}^{l}|^2}\sim\frac{\gamma_{l,l+2}}{\gamma_{l+2}},$$

at least for l such that $\omega l^3/3\leqslant 1$ (to estimate the matrix elements here we make use of the simple analytic approxima-

tions of Ref. 19). According to this criterion for extending the range of observed l, ω_f must decrease, i.e., the intermediate level (occupied by the probe field) must be a sufficiently high "0" level. For example, in the transition from a hydrogen $4p$ level to the vicinity of $n=9$ with subsequent ionization (for $\omega_f \approx 0.025$), the appearance of an h electron ($l=5$) is extremely advantageous.

The subsequent abrupt decrease in the contribution of photoelectrons with large l can be accounted for by slowing of the migration of populations along the chain of levels, resulting from a weakening of the $\gamma_{l,l+2}$ coupling between corresponding Rydberg states.

Taken as a whole, the line intensities at these resonances (and to produce these lines, it is no longer crucial, as can be seen from (20) and (22), that the energy $-1/(2n^2)$ be close to the intermediate level $E_0+\omega_f$) is a factor γ^2 below the intensity I_n [see Eq. (19)] of transitions via the strongly perturbed Rydberg states,

$$I_n^{(l)} \sim \frac{\gamma}{\nu^3} |V_{i0}|^2. \tag{24}$$

Since resonances from weakly perturbed Rydberg states are not critical to the mechanism whereby they are excited from the lower level, however, they can be propagated to much higher energies, i.e., high-l electrons can be generated over the full range $0<E<\omega_f$ of the atomic Rydberg states.

Unfortunately, we cannot even qualitatively compare our results with those reported recently in Ref. 20, where high-l electrons were produced in a pulsed mode by the ionization of atomic hydrogen from the $2s$ level via np states, as the computational data in that paper applied to much stronger fields than those considered here.

5. MULTIPHOTON IONIZATION IN STATES WITH $l \leqslant 2$ AND NO ORBITAL DEGENERACY

Consider now a situation typical of the alkali metals, in which states with $l \leqslant 2$ cannot sustain orbital degeneracy. Assume that the quantity $a=Q/\varepsilon_0$ characterizing the field-induced perturbation of the s and d levels is of the order of the d-level quantum defect ($\mu_2 \sim 10^{-2}-10^{-3}$). Then the s state (with $\mu_0 \gg \mu_2$) can be considered to be shut out of the process, and we can write the probability amplitude for transitions to the continuum with $l=5$ and $l=7$ in the form

$$T_{0p}^{(l=5)} = \frac{t_{02}t_{23}(t_{3p}\tilde{z}_4 - t_{4p}t_{34})}{D},$$

$$T_{0p}^{(l=7)} = \frac{t_{02}t_{23}t_{37}t_{45}}{D}, \tag{25}$$

where

$$D=(z+\tan \pi\mu_2 + i\gamma_2 - t_{02}^2/\varepsilon_0)[(z+i\gamma_3)(z+i\gamma_4) - t_{34}^2] - t_{23}^2(z+i\gamma_4),$$

(here $z=\tan \pi\nu$, $\mu_2 \ll 1$).

We see from (25) that a steep increase in the production of high-l photoelectrons ($l=5,7$) is to be expected when the quantum defect of the d state is balanced by a laser-induced level shift, i.e., when

$$\tan \pi\mu_2 = \frac{t_{02}^2}{\varepsilon_0}. \tag{26}$$

With $l \leqslant (3/\omega_f)^{1/3}$, the ionization probability at the resonant peak is, according to (25),

$$|B_{0p}^{(l\geqslant 5)}| \sim \frac{t_{02}^2}{\varepsilon_0 \gamma}, \tag{27}$$

which agrees to order of magnitude with the ionization probability in the most favorable resonant channels. This also holds for the integrated line intensity at the frequency defined by (26), but only in one of the n levels, since in an off-resonance situation

$$|B_{0p}^{(l\geqslant 5)}| \sim \left[\left(\frac{t_{02}^2}{\varepsilon_0} - \tan \pi\mu_2\right)^2 + \gamma^2\right]^{-1}. \tag{28}$$

The high-l harmonic generation regime considered here thus requires that special conditions be present if it is to realized.

6. CONCLUSIONS

To summarize, we list several conclusions that bear on the characteristics of the processes examined here, averaged of the energy interval $0<E<\omega_f$, assuming that V_{i0} is independent of Ω as the latter varies within that interval.

1. With the highest probability, electrons are ejected into photoionization continua via resonant channels $E_n=\omega_f - 1/2(n-\mu)^2$ with $\mu \neq 0$ (and these are precisely the highly perturbed states in which stabilization is observed as $\mu \to \pm 1/2$). The total contribution from these resonances is

$$\bar{I}_1 = \pi |V_{i0}|^2 \frac{|t_{01}t_{1p}+t_{02}t_{2p}|^2}{\gamma_\Sigma (t_{01}^2+t_{02}^2)} \tag{29}$$

for photoelectrons with $l=1$ and $l=3$.

2. According to (20), for photoelectrons with $l=1$ and $l=3$, there is also a nonresonant photoabsorption band with $W=\pi|V_{i0}|^2[Q^2/(t_{01}^2+t_{02}^2)^2]$, for which the corresponding total probability is

$$\bar{I}_2 = \pi |V_{i0}|^2 \frac{Q^2}{(t_{01}^2+t_{02}^2)^2}\,\omega_f. \tag{30}$$

3. Electrons with $l>3$ enter the continuum via resonant channels with $E_n=\omega_f - 1/2n^2$, which duplicate the position of the unperturbed Coulomb levels. To order of magnitude, the intensity is then

$$\bar{I}_3 \sim \pi |V_{i0}|^2 \omega_f \tag{31}$$

(with $\omega_f l^3/3 \leqslant 1$, for which $\gamma_{l,l+2}$, γ_l, and γ_{l+2} are all of the same order of magnitude).

4. For atoms with no orbital degeneracy when $l \leqslant 2$, which is true of the alkali metals, photoelectrons with high angular momentum $l \leqslant n$ can be produced efficiently only under the special circumstances specified by (26). In contrast to the stabilization effect described above, which is observed when $a \gg 1$ [see (16)], the production of high-momentum electrons requires that a modest quantum defect in the d state (as occurs in Li, Na, and K, for example) be canceled by a

laser-induced shift of the level, which is essentially equivalent to $a \ll 1$. In a Na atom ($\mu_2=0.013$), for instance, that is excited via the scheme depicted in Fig. 1 at an external field frequency $\omega_f \sim 0.12$ (near resonance between the levels $n_0=2$ and $n=9$), this takes place for levels $n=7,8,9$ at $f=3.8\cdot 10^6$ V/cm, $f=2.7\cdot 10^6$ V/cm, and $f=1.5\cdot 10^6$ V/cm, which is appreciably less than the field strength required for the stabilization effect to be observable (under these same conditions, the corresponding levels begin to narrow at $f=1.6\cdot 10^7$ V/cm; see Fig. 3).

This work was supported by the Russian Fund for Fundamental Research (Project Nos. 93-03-4700 and 94-03-08896).

[1] M. Gavrila and J. Z. Kominsky, Phys. Rev. Lett. **52**, 619 (1984).
[2] R. M. Potvliege and R. Shakenhaft, Phys. Rev. A **40**, 306 (1985).
[3] M. Dorr, R. Potvliege, D. Proulx *et al.*, Phys. Rev. A **43**, 3729 (1991).
[4] A. Scrinzi, N. Elander, and B. Piraux, Phys. Rev. A **48**, R2527 (1993).
[5] N. B. Delone and V. P. Kraĭnov, Atoms in Strong Optical Fields [in Russian], Énergoizdat, Moscow (1984).
[6] L. P. Rapoport, B. A. Zon, and N. L. Manakov, *Theory of Multiphoton Processes in Atoms* [in Russian], Atomizdat, Moscow (1978).
[7] M. V. Fedorov, *Electrons in Strong Optical Fields* [in Russian], Nauka, Moscow (1981).
[8] I. Ya. Berson, Zh. Eksp. Teor. Fiz. **83**, 1276 (1982) [Sov. Phys. JETP **56**, 731 (1982)].
[9] A. S. Vartazaryan, G. K. Ivanov, and G. V. Golubkov, Opt. Spektrosk. **63**, 557 (1989).
[10] A. M. Movsesyan and M. B. Fedorov, Zh. Eksp. Teor. Fiz. **99**, 411 (1991) [Sov. Phys. JETP **72**, 228 (1991)].
[11] Q. Su, H. Eberly, and J. Javanien, Phys. Rev. Lett. **64**, 862 (1990).
[12] G. K. Ivanov and G. V. Golubkov, Zh. Eksp. Teor. Fiz. **99**, 1404 (1991) [Sov. Phys. JETP **72**, 783 (1991)].
[13] A. Giusti-Suzor and P. Zoller, Phys. Rev. A **36**, 5178 (1987).
[14] G. K. Ivanov, Chem. Phys. Lett. **132**, 89 (1987).
[15] G. K. Ivanov, A. S. Vartazaryan, and G. V. Golubkov, Dokl. Akad. Nauk SSSR **303**, 390 (1988).
[16] G. V. Golubkov and G. K. Ivanov, Zh. Eksp. Teor. Fiz. **104**, 3334 (1993) [Sov. Phys. JETP **77**, 574 (1993)].
[17] V. S. Lisitsa and S. I. Yakovlenko, Zh. Eksp. Teor. Fiz. **66**, 1981 (1974) [Sov. Phys. JETP **39**, 975 (1974)].
[18] R. Grobe, G. Leuchs, and K. Rzezevski, Phys. Rev. A **34**, 1188 (1986).
[19] S. P. Goreslavskiĭ, N. B. Delone, and V. P. Kraĭnov, Zh. Eksp. Teor. Fiz. **82**, 1789 (1982) [Sov. Phys. JETP **55**, 1032 (1982)].
[20] E. Huens and B. Piraux, Phys. Rev. A **47**, 1568 (1993).

Translated by Marc Damashek